Non-singular transitions between assembly modes of 2-DOF planar parallel manipulators with a passive leg

Fabio DallaLibera[1], Hiroshi Ishiguro

Department of Systems Innovation, Osaka University,
1-3 Machikaneyama, Toyonaka, Osaka, Japan

Abstract

In the field of parallel manipulators, the possibility of changing assembly mode without passing through a singular configuration is well known. This kind of transitions was studied in detail for planar 3-DOF manipulators. This paper focuses on 2-DOF parallel manipulators actuated by two RRR legs and constrained to a 2-DOF motion by a passive leg. It first shows that when the platform movement is constrained to rotations and translations along a single direction, nonsingular assembly mode transitions are possible. The direct and inverse kinematic problems of the mechanism are solved. The singularity conditions are written in explicit form and geometrically interpreted. Numerical examples of nonsingular assembly mode transitions are then given. Subsequently, the paper proves that if the platform is instead constrained to translational motions, nonsingular assembly mode transitions become impossible. Remarks on the generalization of the results to a wider class of 2-DOF planar manipulators are finally given.

Keywords: parallel manipulators, nonsingular assembly mode transitions

1. Introduction

In the last decades, parallel robots received growing attention. The high power and accuracy that can be achieved with this kind of structures was exploited in many contexts, ranging from their early application to flight

Email address: fabio.dl@irl.sys.es.osaka-u.ac.jp (Fabio DallaLibera)
[1]Research Fellow of the Japan Society for the Promotion of Science

simulators [1] and tire testing [2] to their more recent use in haptic devices [3] or palletizing [4, 5].

Parallel manipulators are particularly interesting from a theoretical point of view as well [6, 7, 8]. For many aspects, parallel manipulators turn out to be dual to serial manipulators [9, 10], and this can often be explained by the duality between twist and wrench [11]. One particularly interesting concept, observed both in serial and parallel robots, is the possibility of executing nonsingular transitions. It was shown that for some robots, it is possible to pass from one inverse solution to the other *without* passing through a singular configuration [12, 13]. This kind of transitions is possible in presence of a triple solution, which, when projected over the workspace, appears as a cusp point. For this reason, these robots are commonly called cuspidal [14].

A dual phenomenon can be observed for parallel robots. Transitions between different assembly modes can occur without passing through direct kinematic singularities [15, 16]. Also in this case, trajectories that circle cusps in the joint space may correspond to movements that lead to nonsingular transitions between different assembly modes [17]. We note that encircling a cusp point is not the only possible way of obtaining a nonsingular transition between different assembly modes. Indeed, it was shown that it may suffice to encircle an α-curve in the joint space [18]. Nonsingular transitions have both theoretical and practical importance. On the one hand, there may be a strong desire to avoid these nonsingular transitions for being sure that given an actuator configuration the joint configuration is unique, i.e. for remaining in the same uniqueness domain [19]. On the other hand, it may be possible to exploit nonsingular assembly mode transitions to enlarge the workspace [20].

Nonsingular assembly mode transitions were often studied in the case of planar manipulators. These manipulators received particular attention [21, 22, 23, 24, 25, 26] because, besides the inherent interesting potential application in planar motion systems [27], they can provide insights on the more complex case of spatial manipulators [17].

The presence of nonsingular assembly mode transitions was deeply studied for $3-R\underline{P}R$ manipulators [17, 28, 29, 30, 31]. Special attention was given to the cases of equilateral platform [18], similar base and platform [32], and congruent base and platform [33, 34]. The study of the nonsingular transitions was often conducted by keeping one of the joints fixed [29, 27]. Recently, a complete characterization of the cusp points in the 3-D joint space was provided as well [35]. Another commonly studied manipulator is the $3-RRR$ one [36], especially the one with equilateral base and platform [37]. Also in

this case, nonsingular assembly mode transitions were confirmed [38]. Further works dealt with the $3-\underline{P}RR$ manipulator, studied in [18] and [39], the $R\underline{P}R-2-PRR$, examined in [40], and other configurations employing only rotational joints [41].

Much less literature can be found for 2-DOF mechanisms. Most literature focuses on the $RRRRR$ configuration [21, 42, 43, 44, 45, 46]. Prismatic joints may be used for the joint proximal to the base or for the central joints, obtaining a $PRRRP$ manipulator [47] or a $RPRPR$ configuration [24], respectively. More recently, parallelogram based structures found application as well [48, 49]. To the best of our knowledge, nonsingular assembly mode transitions were never shown for 2-DOF manipulators, excluding the case of 3-DOF manipulators with one joint fixed, for which the platform usually undergoes compound translations and rotations.

This paper investigates the possibility of executing nonsingular assembly mode transitions in simpler cases. First, it shows the possibility of executing such maneuvers for a 2-DOF manipulator whose platform is actuated by $\underline{R}RR$ legs and constrained to rotations and translations along a single direction by a passive leg. The structure is described in Section 2. The solution to the inverse and direct kinematics problems is given in Section 3 and Section 4, respectively. Singularities are then analyzed in Section 5. Their geometrical interpretations is given, and the singularity loci is obtained. A nonsingular assembly mode transition, obtained by encircling one of the cusps present in the loci, is then presented in Section 6. Successively, a modified version of the manipulator, that allows only translational movements, is introduced in Section 7. The impossibility of executing nonsingular assembly mode transitions with this manipulator is proved. Section 8 then introduces a purely translational mechanisms that exhibit nonsingular assembly mode transitions. Section 9 summarizes the results and discusses possible extensions of the work presented in this paper.

2. Kinematic structure

In the field of 2-DOF planar parallel manipulators, focus is usually given to manipulators in which both the degrees of freedom are purely translational. Conversely, this paper first introduces a manipulator capable of platform reorientation and displacement along a single direction. This kind of structure may be considered as the planar version of lower mobility spatial

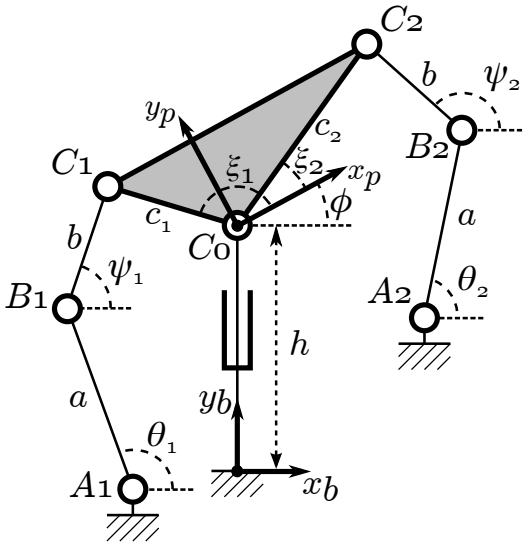

Figure 1: The 2-RRR-PR manipulator studied.

parallel manipulators that employ passive legs between the base and the platform [50, 51].

The link configuration is presented in Fig 1. The two links of length $a \gneqq 0$ are input links and the joints A_1 and A_2 are the only actuated joints. These links are connected to the platform through the links B_iC_i of length $b \gneqq 0$. Without loss of generality, the prismatic joint axis of the passive leg is taken as the vertical axis of the base reference frame. The location of the actuated joints A_1 and A_2 is denoted in this reference frame by $(o_{x,1}, o_{y,1})$ and $(o_{x,2}, o_{y,2})$, respectively. The input variables, i.e. the angles formed by the links A_iB_i with the horizontal axis, are denoted by θ_i, $i \in \{1, 2\}$. The angles[2] formed between the horizontal and the B_iC_i links are denoted by ψ_i, $i \in \{1, 2\}$.

The reference frame for the platform is an arbitrary frame with the origin located at C_0, the rotational joint that connects the passive leg to the platform. The position, in the platform reference frame, of the rotational joints C_1 and C_2 is denoted for convenience in polar coordinates, (c_i, ξ_i), $i \in \{1, 2\}$, $c_i \gneqq 0$. The orientation of the platform with respect to the reference frame is denoted by ϕ, and its displacement along the vertical by h.

[2]In the following, figures included, all angles are assumed to be expressed in radians.

3. Inverse kinematics

From Fig. 1 the following loop closure equations can be written

$$\begin{aligned} c_i cos\left(\phi+\xi_i\right) - o_{x,i} - a\cos\left(\theta_i\right) &= \quad b\cos\left(\psi_i\right) \\ h + c_i sin\left(\phi+\xi_i\right) - o_{y,i} - a\sin\left(\theta_i\right) &= \quad b\sin\left(\psi_i\right). \end{aligned} \tag{1}$$

Defining

$$\begin{aligned} d_{x,i} &= c_i cos(\phi+\xi_i) - o_{x,i} \\ d_{y,i} &= h + c_i sin(\phi+\xi_i) - o_{y,i} \\ d_i^2 &= d_{x,i}^2 + d_{y,i}^2, \end{aligned}$$

then squaring and summing the equations we obtain

$$d_i^2 - 2d_{x,i}a\cos(\theta_i) - 2d_{y,i}a\sin(\theta_i) + a^2 = b^2. \tag{2}$$

If $d_i \neq 0$ then by rearranging the terms, and dividing by $2d_ia$, we can write

$$\frac{d_i^2 + a^2 - b^2}{2d_ia} = \frac{d_{x,i}}{d_i}\cos(\theta_i) + \frac{d_{y,i}}{d_i}\sin(\theta_i)$$

The right hand side can be interpreted as the expansion of the cosine of a difference, and therefore[3]

$$\theta_i = \arctan_2(d_{y,i}, d_{x,i}) \pm \arccos\left(\frac{d_i^2 + a^2 - b^2}{2d_ia}\right). \tag{3}$$

We notice that we have

- one solution when $\frac{d_i^2+a^2-b^2}{2d_ia} = -1$, which is verified when the arm is fully-stretched ($b = d_i + a$), and when $\frac{d_i^2+a^2-b^2}{2d_ia} = 1$, corresponding to the arm folded back ($b = d_i - a$).
- no solution for $\left|\frac{d_i^2+a^2-b^2}{2d_ia}\right| > 1$, i.e. for $b < d - a$ or $b > d + a$.
- two solutions for $\left|\frac{d_i^2+a^2-b^2}{2d_ia}\right| < 1$, corresponding to the "elbow-up" and "elbow-down" solutions.

[3] $\arctan_2$ is the two-argument arctangent function that corrects for the quadrant of the angle, $\arctan_2(y,x) = 2\arctan\frac{y}{\sqrt{x^2+y^2}+x}$.

It is therefore clear that the manipulator has four working modes, given by the elbow-up / elbow-down configuration of each of the two legs.

When one of the d_i is zero, $i \in \{1, 2\}$ then the system for that leg reduces to

$$a\cos(\theta_i) = b\cos(\theta_i)$$
$$a\sin(\theta_i) = b\sin(\theta_i)$$

which has no solutions for $a \neq b$ and infinite solutions otherwise.

4. Direct kinematics

In the direct kinematics, given the values θ_1 and θ_2, we want to determine the possible outputs ϕ and h, $-\pi < \phi \leq \pi$. When the actuated joints are locked, the structure can be thought as a four bar linkage to which the passive constraining leg is added. The coupler curve of a four bar linkage is a sextic, we can therefore expect the mechanism to have degree 6 or less.

Using the Weierstrass substitution $t = \tan(\phi/2)$, an algebraic equation in t of degree 6 can be found, following a derivation similar to the one reported in [52] for the $R\underline{P}R - PR - R\underline{P}R$ manipulator. For a given ϕ, the corresponding (unique) height h is

$$h = \frac{f_2^2 + g_2^2 - f_1^2 - g_1^2}{2(g_1 - g_2)},$$

where

$$f_i = c_i \cos(\phi + \xi_i) - o_{x,i} - a\cos(\theta_i)$$
$$g_i = c_i \sin(\phi + \xi_i) - o_{y,i} - a\sin(\theta_i)$$

when $g_1 \neq g_2$. If $g_1 = g_2$, then it can be shown that the multiplicity of the solutions in ϕ is at least two, and for each value of ϕ there are two solutions for h, namely

$$h = -g_1 \pm \sqrt{b^2 - f_1^2}.$$

We can show that six is a tight bound to the number of solutions by providing examples of mechanism inputs that admit up to 6 different assembly modes. Figure 2 provides an example design (design 1) in which none of the 6 solutions is such that $g_1 = g_2$. Figure 3 provides an example (design 2) in which 4 solutions with $g_1 = g_2$ are present. For this configuration, other two solutions, having the same h, exist. Dimensions of the manipulators and solutions are reported, respectively, in tables 1 and 2.

Parameter	Design 1	Design 2
a	1	1
b	3/4	3/4
c_1	2/3	3/2
c_2	2/3	3/2
ξ_1	$2/3\pi$	π
ξ_2	$\pi/3$	0
θ_1	$\pi/4$	$\pi/3$
θ_2	$2/3\pi$	$2/3\pi$
$\emptyset_{x,1}$	-1	-2/3
$\emptyset_{x,2}$	1	2/3
$\emptyset_{y,1}$	0	0
$\emptyset_{y,2}$	-2/5	-14/5

Table 1: Design dimensions

Design 1		Design 2	
ϕ	h	ϕ	h
-2.99087	0.983679	-1.938	-0.278599
-2.9365	1.34443	-1.938	-0.78935
-1.07736	-0.245183	-1.20359	0.117353
-0.425721	-0.670954	-1.20359	-1.1853
-0.338703	0.782205	-1.97007	-0.533975
0.89563	-0.0481114	-0.934547	-0.533975

Table 2: Design solutions

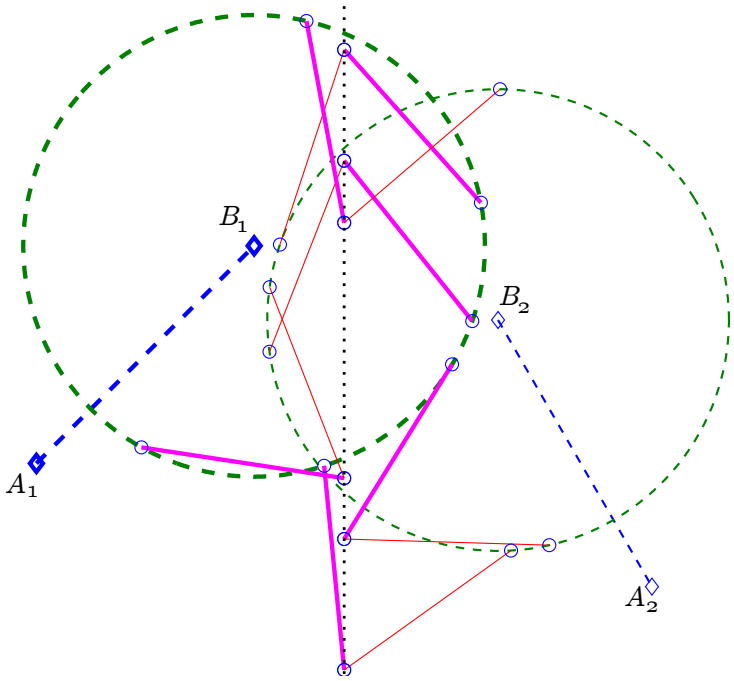

Figure 2: The six direct kinematic solutions of Design 1. The links A_iB_i of length a are shown by dashed lines. The dashed circles have radius b and center B_i. They indicate the possible locations for the platform points C_i in presence of the sole constraint given by links of length b. The dotted line represents the y axis, i.e. the possible locations for C_0. Links A_1B_1, B_1C_1 and the circle of radius b centered in B_1 are shown with thick line. The elements of the second leg are shown with thin line.

5. Singularity analysis

The loop closure equations can be written in vector form as

$$\boldsymbol{h} + \boldsymbol{c}_i = \boldsymbol{o}_i + \boldsymbol{a}_i + \boldsymbol{b}_i$$

for $i \in \{1, 2\}$, where

$$\begin{aligned}
\boldsymbol{h} &= [0 \quad h \quad 0]^T \\
\boldsymbol{c}_i &= [c_{x,i} \quad c_{y,i} \quad 0]^T = c_i[\cos(\phi + \xi_i) \quad \sin(\phi + \xi_i) \quad 0]^T \\
\boldsymbol{o}_i &= [o_{x,i} \quad o_{y,i} \quad 0]^T \\
\boldsymbol{a}_i &= a[\cos(\theta_i) \quad \sin(\theta_i) \quad 0]^T \\
\boldsymbol{b}_i &= b[\cos(\psi_i) \quad \sin(\psi_i) \quad 0]^T.
\end{aligned}$$

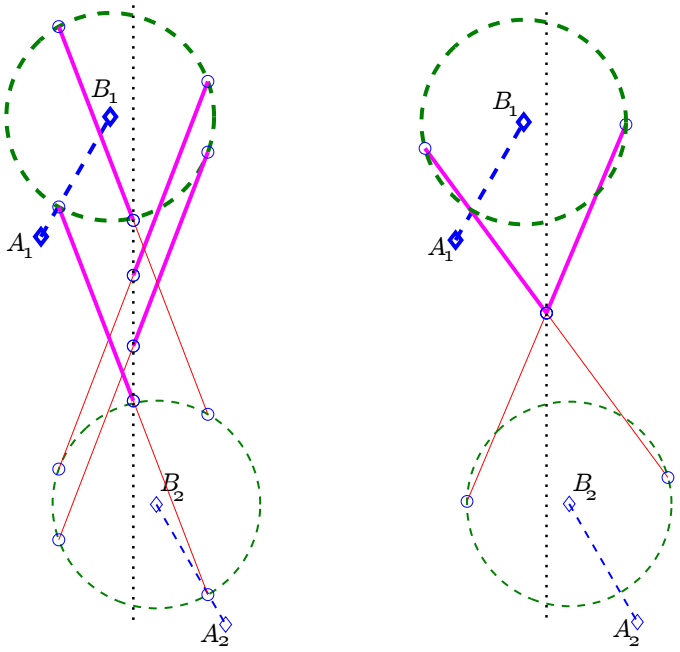

(a) (b)

Figure 3: The six kinematic solutions of Design 2. Note that for this design, the platform points C_1, C_0 and C_2 are aligned. Panel (a) shows 4 direct kinematic solutions for which $g_1 = g_2$. Panel (b) shows the remaining two solutions, which share the same h. The graphical notation of the figures follows that of Fig. 2.

The derivative over time yields

$$\dot{h}\boldsymbol{y} + \dot{\phi}\boldsymbol{z} \times \boldsymbol{c}_i = \dot{\theta}_i \boldsymbol{z} \times \boldsymbol{a}_i + \dot{\psi}_i \boldsymbol{z} \times \boldsymbol{b}_i \tag{4}$$

where $\boldsymbol{y} = [0 \quad 1 \quad 0]^T$ and $\boldsymbol{z} = [0 \quad 0 \quad 1]^T$. Dot multiplication of both members of by $\boldsymbol{b}_i$ leads to

$$\dot{h}\boldsymbol{y} \cdot \boldsymbol{b}_i + \dot{\phi}\boldsymbol{z} \cdot (\boldsymbol{c}_i \times \boldsymbol{b}_i) = \dot{\theta}_i \boldsymbol{z} \cdot (\boldsymbol{a}_i \times \boldsymbol{b}_i),$$

which can be written in matrix form as

$$\boldsymbol{J}_w \dot{\boldsymbol{w}} = \boldsymbol{J}_q \dot{\boldsymbol{q}}$$

with $\boldsymbol{w} = [h \quad \phi]^T$, $\boldsymbol{q} = [\theta_1 \quad \theta_2]^T$ and

$$\boldsymbol{J}_w = \begin{bmatrix} b_{y,1} & b_{y,1}c_{x,1} - b_{x,1}c_{y,1} \\ b_{y,2} & b_{y,2}c_{x,2} - b_{x,2}c_{y,2} \end{bmatrix} = \begin{bmatrix} b\sin(\psi_1) & bc_1 \sin\left(\psi_1 - (\phi + \xi_1)\right) \\ b\sin(\psi_2) & bc_2 \sin\left(\psi_2 - (\phi + \xi_2)\right) \end{bmatrix}$$

$$\boldsymbol{J}_q = \begin{bmatrix} a_{x,1}b_{y,1} - a_{y,1}b_{x,1} & 0 \\ 0 & a_{x,2}b_{y,2} - a_{y,2}b_{x,2} \end{bmatrix} = \begin{bmatrix} ab\sin(\psi_1 - \theta_1) & 0 \\ 0 & ab\sin(\psi_2 - \theta_2) \end{bmatrix}.$$

Inverse kinematic singularities, that is local loss of degrees of freedom, occurs for $\det(\boldsymbol{J}_q) = 0$. This happens for $\psi_i - \theta_i = k\pi$, $k \in \mathbb{Z}$, i.e. when one arm is fully-stretched or folded back.

In order to compute the singularity loci, let us rewrite the loop closure equations (1) under the assumption $\psi_i - \theta_i = k\pi$ as

$$\begin{aligned} o_{x,i} + (a + \kappa_i b)\cos(\theta_i) &= c_i \cos(\phi + \xi_i) \\ o_{y,i} + (a + \kappa_i b)\sin(\theta_i) - h &= c_i \sin(\phi + \xi_i) \end{aligned} \tag{5}$$

where $\kappa_i = 1$ for $\psi_i = \theta_i \bmod 2\pi$ and $\kappa = -1$ for $\psi_i = \theta_i + k\pi \bmod 2\pi$. Squaring and summing the equations we get

$$(o_{x,i} + (a + \kappa_i b)\cos(\theta_i))^2 + (o_{y,i} + (a + \kappa_i b)\sin(\theta_i) - h)^2 = c_i^2$$

from which we derive

$$h = o_{y,i} + (a + \kappa_i b)\sin(\theta_i) + \zeta\sqrt{\Delta_{C,i}} \tag{6}$$

with $\Delta_{C,i} = c_i^2 - (o_{x,i} + (a + \kappa_i b)\cos(\theta_i))^2$ and $\zeta \in \{-1, +1\}$, i.e. for each singular position of the i-th leg (defined by θ_i and κ_i) we have

- no feasible configuration if $\Delta_{C,i} < 0$
- the possibility of having singular platform configurations with a single height if $\Delta_{C,i} = 0$
- the possibility of having two height values if $\Delta_{C,i} > 0$

For each height h of the platform, computed from Eq. 6, the corresponding platform orientation can be computed from the equations (5) as

$$\phi = -\xi_i + \arctan_2\left(o_{y,i} + (a + \kappa_i b)\sin(\theta_i) - h, o_{x,i} + (a + \kappa_i b)\cos(\theta_i)\right).$$

The feasibility of these (h, ϕ) configurations depends on the other leg $3 - i$, for which the number of real solutions of Eq. 3 must be checked. Depending on the number of solutions of this equation, for each platform we then get zero, one (in case both legs are in a singular configuration) or two solutions corresponding to the two working modes of the leg $3 - i$.

Fig. 4 shows the inverse kinematic singularities in the joint space. The legs are non-cuspidal, therefore the serial singularities separate the inverse kinematics solutions. Fig. 5 shows how the singularities delimit the workspace. A direct expression for the workspace limits can be found in the following way. Let us rearrange the loop closure equations as

$$\begin{aligned} c_i \cos(\phi + \xi_i) - o_{x,i} &= b\cos(\psi_i) + a\cos(\theta_i) \\ h + c_i \sin(\phi + \xi_i) - o_{y,i} &= b\sin(\psi_i) + a\sin(\theta_i) \end{aligned} \quad .$$

For a given ϕ, by squaring and summing the two equations we obtain the two solutions for h,

$$h = \mu_{H,i} \pm \sqrt{\Delta_{H,i}}$$

with

$$\begin{aligned} \mu_{H,i} &= o_{y,i} - c_i \sin(\phi + \xi_i) \\ \Delta_{H,i} &= a^2 + b^2 + 2ab\cos(\delta_i) - (c_i \cos(\phi + \xi_i) - o_{x,i})^2 \end{aligned}$$

where $\delta_i = \psi_i - \theta_i$.

Intuitively, the workspace extreme h values are obtained with one of the legs fully stretched, and therefore for one $\delta_i = 0$. This can be proven formally by considering that the partial derivatives of the two solutions with respect to δ_i are respectively

$$\frac{\partial h}{\partial \delta_i} = \mp \frac{ab\sin(\delta_i)}{\sqrt{\Delta_{H,i}}}$$

and therefore the solution $h = \mu_{H,i} + \sqrt{\Delta_{H,i}}$ (resp. $h = \mu_{H,i} - \sqrt{\Delta_{H,i}}$) achieves its maximum (resp. minimum) for $\delta_i = k2\pi$ and its minimum (resp. maximum) for $\delta_i = \pi + k2\pi$. For a given ϕ, therefore, the range of possible heights h is

$$\left[max_i \left\{ \mu_{H,i} - \sqrt{\Delta^*_{H,i}} \right\},\ min_i \left\{ \mu_{H,i} + \sqrt{\Delta^*_{H,i}} \right\} \right]$$

with

$$\Delta^*_{H,i} = (a+b)^2 - (c_i \cos(\phi + \xi_i) - o_{x,i})^2 .$$

Direct kinematic singularities (loss of controllability of at least one degree of freedom) occur for $\det(\boldsymbol{J}_w) = 0$, i.e. for

$$c_2 \sin(\psi_1) \sin(\psi_2 - (\phi + \xi_2)) - c_1 \sin(\psi_2) \sin(\psi_1 - (\phi + \xi_1)) . \qquad (7)$$

We can categorize the singularities into several cases:

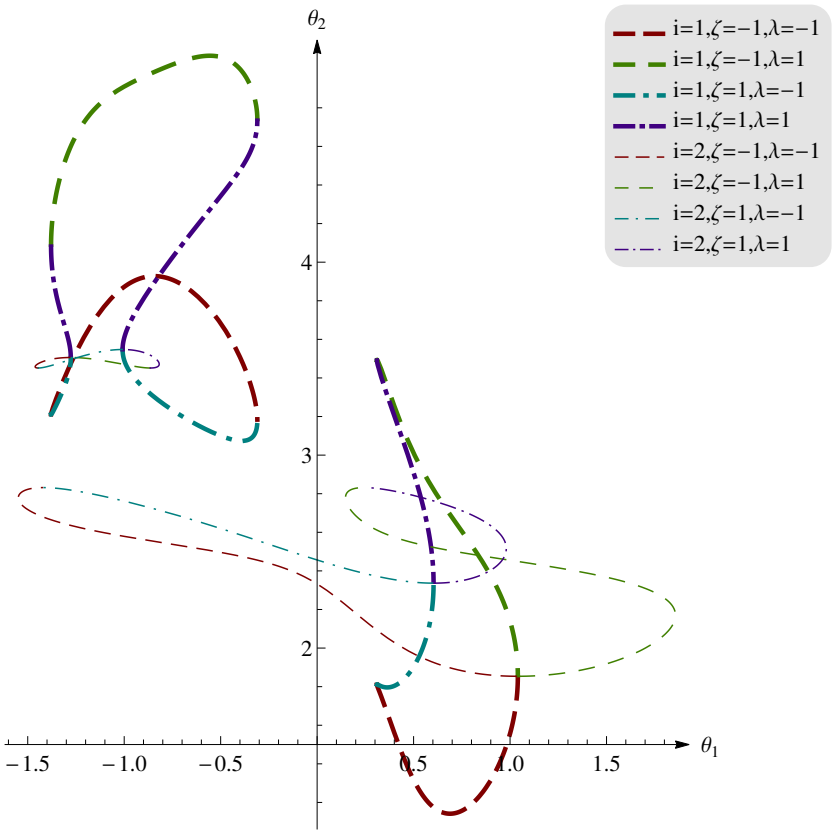

Figure 4: The inverse kinematic singularities in the joint space. Thick lines denote singularities of the first leg ($i = 1$), thin lines show the singularities of the second leg ($i = 2$). The two possible values for the height of the platform associated to a singular solution are shown by dashed lines ($\zeta = 1$) and dash dot lines ($\zeta = -1$). Different dash spacings are used to indicate the working mode of the leg that is not in a singular configuration. Expressing its inverse kinematic solution as $\theta_{3-i} = \arctan_2(d_{y,3-i}, d_{x,3-i}) + \lambda \arccos\left(\frac{d_{3-i}^2+a^2-b^2}{2d_{3-i}a}\right)$, solutions obtained for $\lambda = -1$ are shown by longer spacings and solutions with $\lambda = 1$ are shown by shorter ones. We note that all of the singularities are obtained for $\kappa = 1$, i.e. only singularities with the arm fully stretched, and none with the folded back arm, exist for this particular dimensioning of the manipulator.

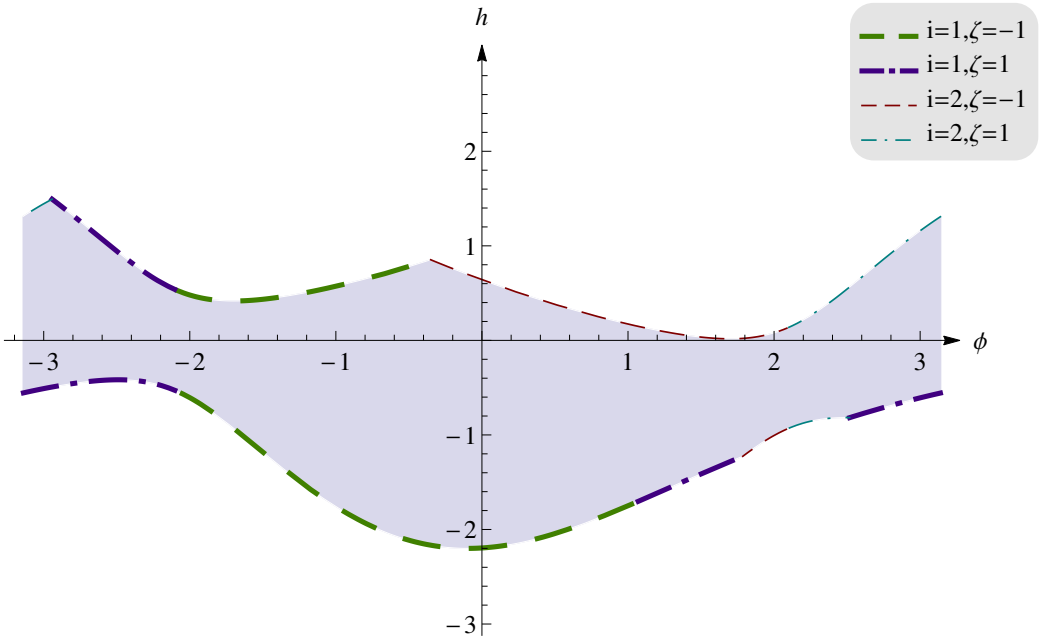

Figure 5: The inverse kinematic singularities in the workspace. Thick lines denote singularities of the first leg, thin lines show the singularities of the second leg. The two possible values for the height of the platform associated to a singular solution are shown by dashed lines ($\zeta = 1$) and dash dot lines ($\zeta = -1$). We note that all of the singularities are obtained for $\kappa = 1$, i.e. only singularities with the arm fully stretched, and none with the folded back arm, exist for this particular dimensioning of the manipulator. The shaded area denotes the reachable workspace.

- $b_{y,i} = 0 \wedge c_{y,i} = 0$, $i \in \{1, 2\}$. In this case, the rank of the matrix is zero, and any infinitesimal movement (rotation of the platform around C_0 and vertical translation) is allowed, see Fig. 6(a).

- $b_{y,1} = b_{y,2} = 0$, $\exists c_{y,i} \neq 0$, $i \in \{1, 2\}$. In this case, the platform does not withstand infinitesimal translations along the vertical axis, see Fig. 6(b).

- $\exists b_{y,i} \neq 0$, $i \in \{1, 2\}$, and $\boldsymbol{b}_i$ collinear with $\boldsymbol{c}_i$. In this case of singularity, by Eq. 7, $\boldsymbol{b}_{3-i}$ is collinear with $\boldsymbol{c}_{3-i}$ as well, and the platform can undergo infinitesimal rotations around C_0, see Fig. 6(c).

- $\exists b_{y,i} \neq 0$, $i \in \{1, 2\}$, and $\boldsymbol{b}_i$ not collinear with $\boldsymbol{c}_i$. In this case, under the conditions of Eq. 7, the platform cannot withstand a rototranslation movement with $\dot{h} = \alpha(b_{y,i}c_{x,i} - b_{x,i}c_{y,i})$ and $\dot{\phi} = -\alpha b_{y,i}$, where α is an arbitrary constant, $\alpha \in \mathbb{R}$, $\alpha \neq 0$, see Fig. 6(d).

The direct kinematic singularities are shown in the joint space and in the workspace in Fig. 7 and Fig. 8, respectively.

6. Nonsingular transition

The projection of the direct kinematic singularities over the joint space, visible in Fig. 7, clearly shows a cusp in proximity of the configuration $(\theta_1, \theta_2) = (1, 1.65)$. We note that there are other cusps, and that actually the number of cusps depends on the dimensioning of the manipulator. It can be shown, for instance, that there exists particular dimensionings that have no cusps at all. Analysis of the number of cusps, as provided in [53] for the $3 - R\underline{P}R$ manipulator, may be of great interest for a deeper understating of this class of manipulators. In the following, however, we just focus on the analysis of this single cusp and show that it allows the execution of nonsingular assembly mode transitions.

Three dimensional projections of the direct kinematic solutions in the neighborhood of this cusp are shown in Fig. 9 and Fig. 10. Fig. 9 shows the projection over θ_1, θ_2, ϕ. In this space, the configuration manifold has a typical S-shaped folding [17]. Fig. 10 shows the projection over θ_1, θ_2, h.

A nonsingular transitions between two assembly modes can be executed by encircling this cusp. In particular, it is possible to encircle the cusp by a very elementary manipulator actuation: a pure rotation of the platform

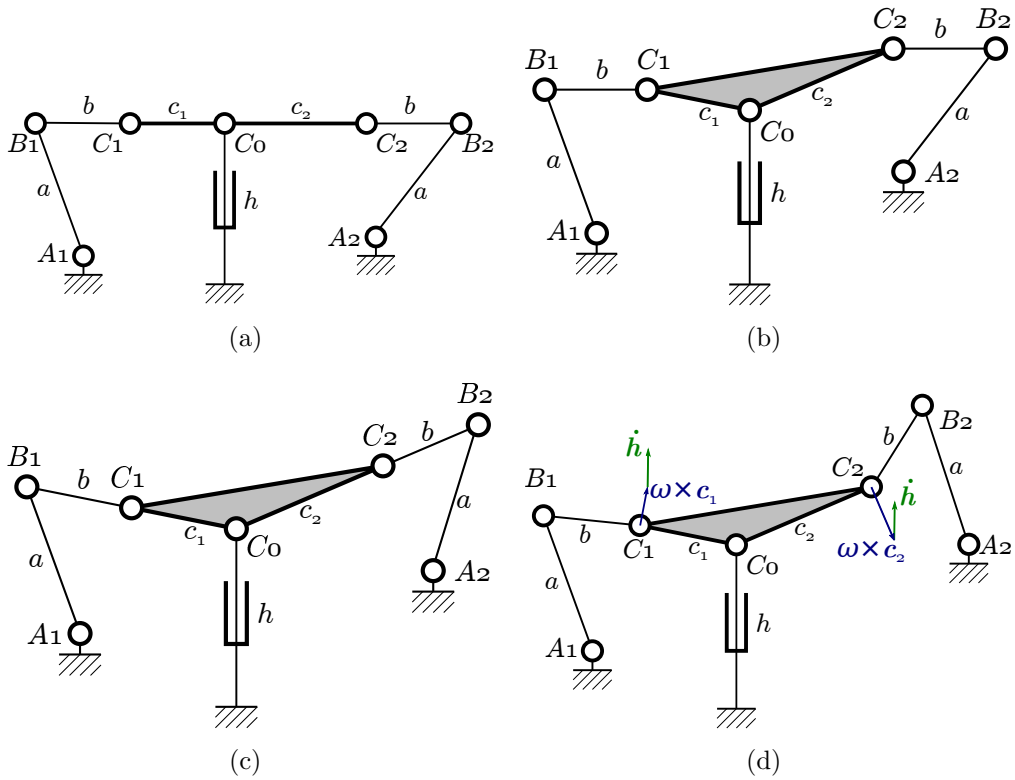

Figure 6: Geometrical interpretation of the direct kinematic singular configurations. (a) The platform can perform any infinitesimal rototranslation. (b) The platform can undergo infinitesimal translations. (c) The platform can undergo infinitesimal rotations around C_0. (d) The platform cannot withstand infinitesimal rototranslations with a specific ratio between the rotation and the translation velocities $\dot{h}$ and $\dot{\phi}$, respectively. In particular, this ratio makes the instantaneous velocity of each point C_i, $\dot{\boldsymbol{h}} + \boldsymbol{\omega} \times c_i = \dot{h}\boldsymbol{y} + \dot{\phi}\boldsymbol{z} \times \boldsymbol{c}_i$, orthogonal with the respective link b_i. A numerical example for this case is $a = 3$, $b = 2$, $\theta_1 = \theta_2 = 2/3\pi$, $c_1 = 2$, $\xi_1 = 5/6\pi$, $c_2 = 3$, $\xi_2 = \pi/6$, $o_{x,1} = 3/2 - \sqrt{3} - \frac{7}{\sqrt{13}}$, $o_{x,2} = 3/2 + \frac{3\sqrt{3}}{2} + \frac{1}{\sqrt{7}}$, $o_{y,1} = 1 + \sqrt{3/13} - \frac{3\sqrt{3}}{2}$, $o_{y,2} = 3/14(7 - 7\sqrt{3} + 2\sqrt{21})$ $\phi = 0$, $h = 0$.

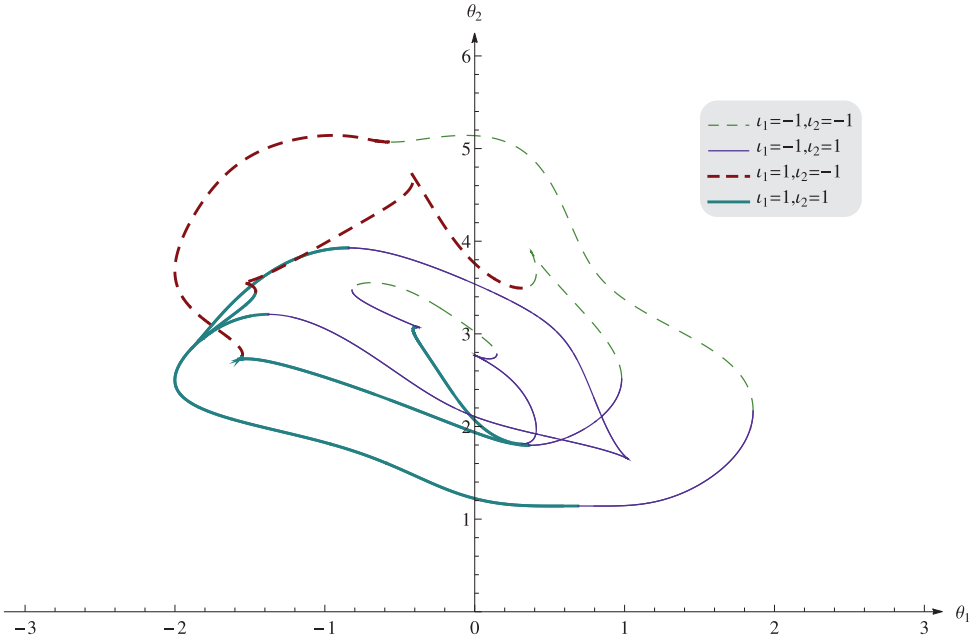

Figure 7: The direct kinematic singularities in joint space. Different line styles are used for different working modes. In particular, by defining the inverse kinematic solutions as $\theta_i = \arctan_2(d_{y,i}, d_{x,i}) + \iota_i \arccos\left(\frac{d_i^2+a^2-b^2}{2d_i a}\right)$, $\iota_i \in \{-1, 1\}$, $i \in \{1, 2\}$, working modes with $\iota_1 = -1$ are shown with thin lines, while working modes with $\iota_1 = 1$ are shown by thick lines. Working modes with $\iota_2 = -1$ are shown by dashed lines, $\iota_2 = 1$ are shown by solid lines.

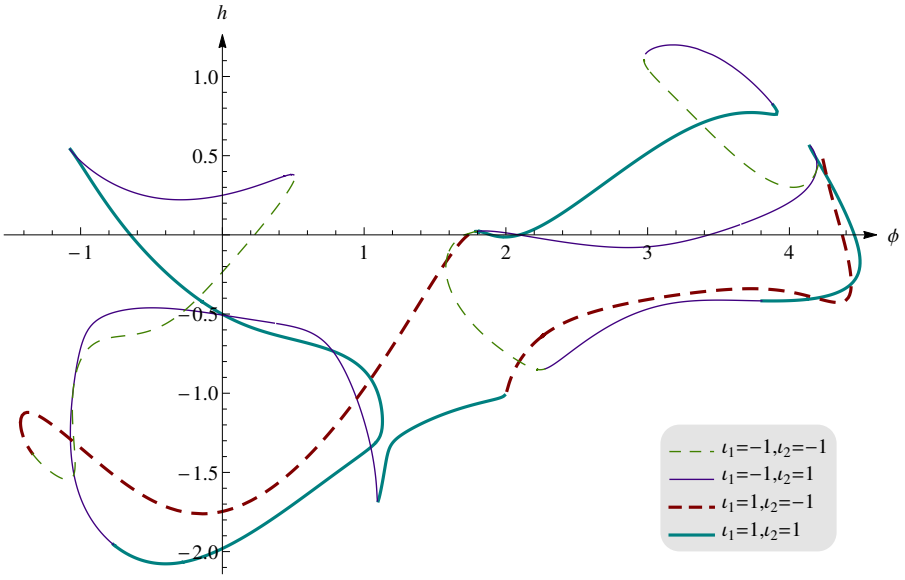

Figure 8: The direct kinematic singularities in the workspace. Different line styles are used for different working modes, with the criteria explained in Fig. 7.

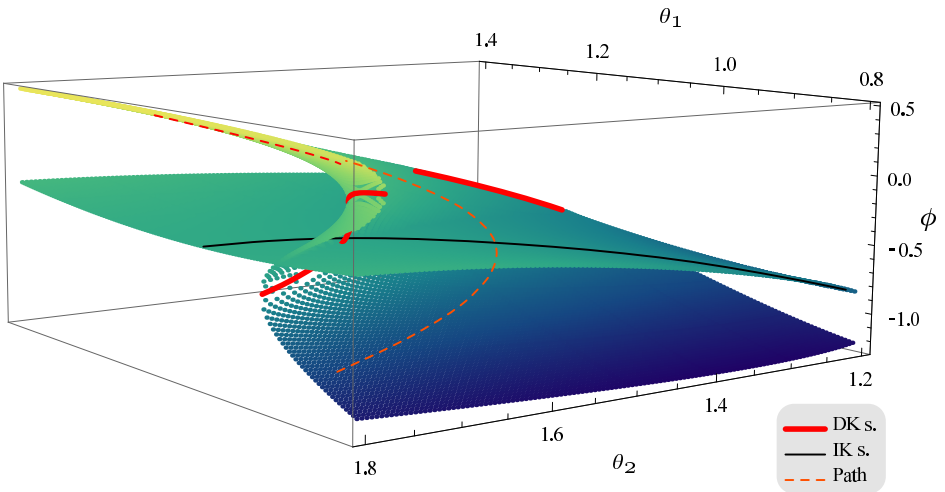

Figure 9: The projection of the manipulator configurations over the θ_1, θ_2, ϕ space. Thick lines indicate direct kinematics singularities. Thin solid lines indicate inverse kinematics singularities. The dashed line shows the path taken during the nonsingular maneuver.

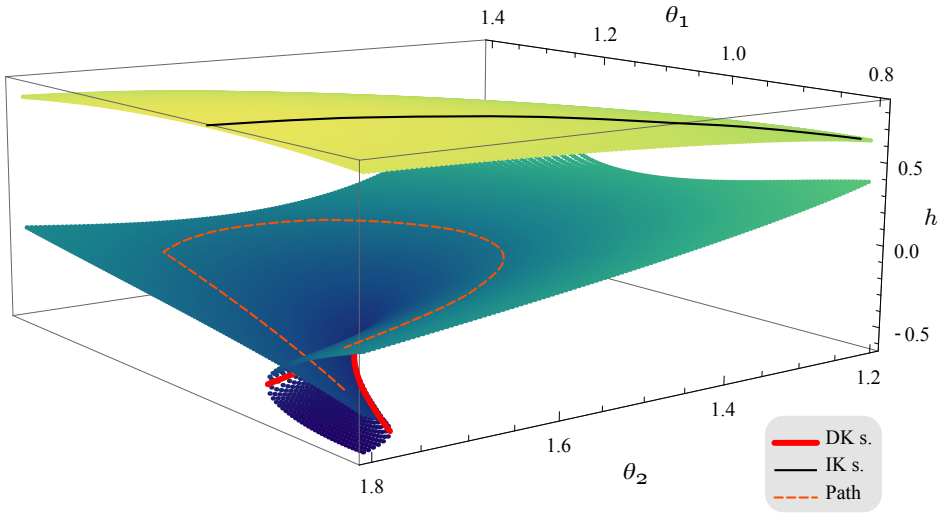

Figure 10: The projection of the manipulator configurations over the θ_1, θ_2, h space. Thick lines indicate direct kinematics singularities. Thin solid lines indicate inverse kinematics singularities. The dashed line shows the path taken during the nonsingular maneuver.

around C_0 followed by a pure translation in the vertical direction. The movement is planned in the workspace, and connects two configurations having the same value for the actuated joints. In more detail, for $(\theta_1, \theta_2) = (0.87, 1.77)$, four platform configurations (ϕ, h) are feasible, namely $(-0.9917, -0.1942)$, $(0.3198, -0.4153)$, $(-0.3255, 0.8265)$ and $(-0.0922, -0.5873)$. The first two configurations can be connected by a movement that first changes the orientation ϕ, and than changes the platform height h. Fig. 11 and Fig. 12 show the evolution of the variables, assuming each movement section is executed taking 50 arbitrary time units. Fig. 12 also reports the value of the the determinants of $\boldsymbol{J}_q$ and $\boldsymbol{J}_w$ for each configuration, showing that no singularity is encountered during the maneuver. We note that since each leg of the manipulator is non-cuspidal, by checking that no inverse kinematic configuration are passed, we are guaranteed that the working mode does not change during the assembly mode transition. Fig. 13 shows some of the postures taken by the manipulator during the nonsingular assembly mode transition.

7. Translational version

Fig. 14(a) shows a purely translational 2-DOF manipulator obtained by a very simple modification of the structure previously studied. In detail,

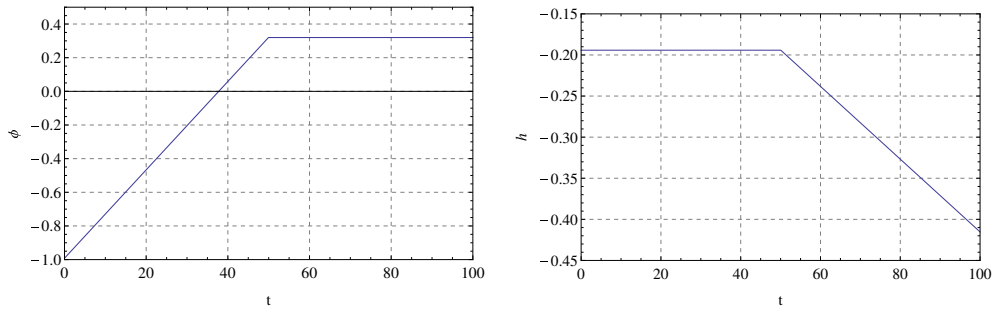

(a) (b)

Figure 11: Nonsingular assembly transition. Evolution over time of the platform orientation in panel (a) and of its height in panel (b).

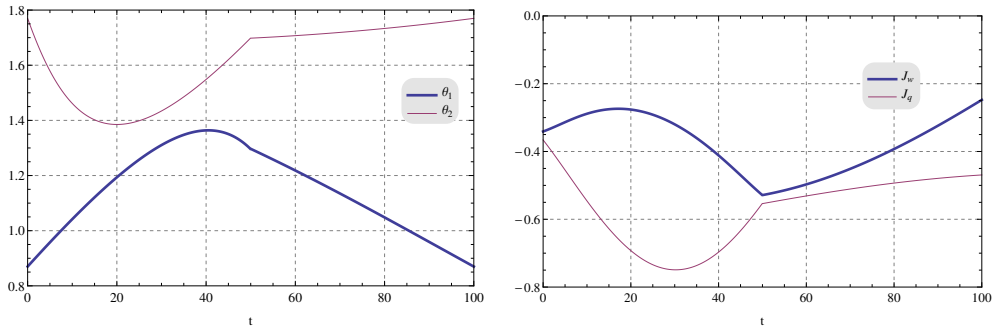

(a) (b)

Figure 12: Nonsingular assembly transition. (a) Evolution over time of the actuated joint angles. Thick line is used to indicate the value of θ_1, thin line shows the value of θ_2. (b) Evolution of the determinants of $\boldsymbol{J}_w$ (thick line) and $\boldsymbol{J}_q$ (thin line) used for identifying direct and inverse kinematic singularities, respectively.

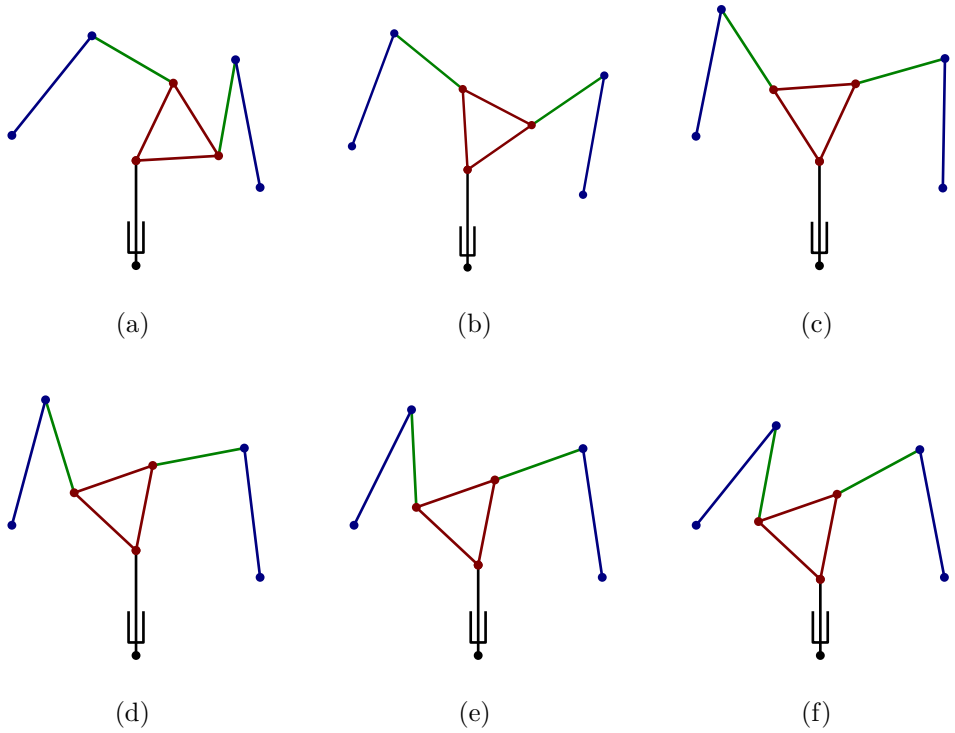

Figure 13: Poses assumed during the nonsingular assembly mode transition. (a) Initial configuration ($t = 0$). (b) Configuration with minimum θ_2 ($t \approx 20.5$). (c) Configuration with maximum θ_1 ($t \approx 40.5$). (d) Configuration at the end of the platform rotation. (e) Generic configuration during the platform vertical descend movement($t = 75$). (f) Final configuration ($t = 100$).

the rotational joint of the passive leg is replaced with a prismatic joint not parallel with the already existing "vertical" prismatic joint. A very natural choice would be making the prismatic joints orthogonal. A more practically oriented variant of the mechanism is shown in Fig. 14(b). We note that this manipulator is similar to the $RPRPR$ [24].

In the following, we will show that despite the similarity with the previous manipulator, this structure cannot undergo nonsingular assembly mode transitions. This is not a unique case in the realm of parallel manipulators, see for instance [54]. For simplifying the notation and without loss of generality, the reference frame for the base is taken in A_1. The coordinates of C_1 are denoted by (x, y) and are taken as the reference for the platform position (output variables). The axes of this platform reference frame are

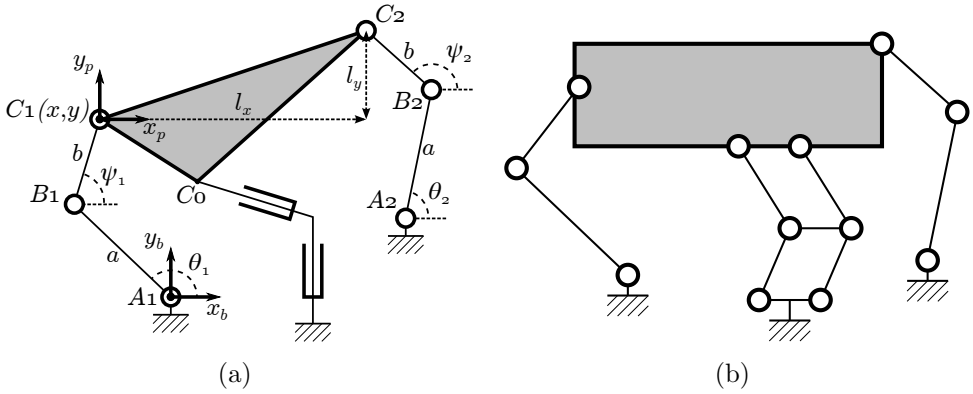

Figure 14: (a) The 2-RRR-PP purely translational manipulator obtained by substitution of the rotational joint with a prismatic joint. (b) A more practical variant, realized only with rotational joints and with improved stiffness due to the parallel configuration of the constraining linkage.

assumed parallel to the ones of the base reference frame. The location of C_2 is expressed in the platform reference frame by the coordinates (l_x, l_y). The actuated joints remain located in A_1 and A_2, having in this case coordinates $(0, 0)$ and $(o_{x,2}, o_{y,2})$, respectively. The length of the links proximal to the actuated joints is still denoted by $a \gneqq 0$, and the more distal links have once again length $b \gneqq 0$.

Given this notation, the loop closure equations are reduced to

$$\begin{aligned} a\cos(\theta_1) + b\cos(\psi_1) + l_x &= o_{x,2} + a\cos(\theta_2) + b\cos(\psi_2) \\ a\sin(\theta_1) + b\sin(\psi_1) + l_y &= o_{y,2} + a\sin(\theta_2) + b\sin(\psi_2). \end{aligned}$$

The solution of the direct kinematics problem for this manipulator can be found using an approach very close to the derivation of Eq. 3. By defining

$$\begin{aligned} \rho_x &= a\cos(\theta_1) - a\cos(\theta_2) + l_x - o_{x,2} \\ \rho_y &= a\sin(\theta_1) - a\sin(\theta_2) + l_y - o_{y,2} \\ \rho &= \sqrt{\rho_x^2 + \rho_y^2} \end{aligned}$$

the equations can be rewritten as

$$b\cos(\psi_1) + \rho_x = b\cos(\psi_2) \tag{8}$$

$$b\sin(\psi_1) + \rho_y = b\sin(\psi_2) \tag{9}$$

from which, by squaring each term of the equations and summing, we obtain

$$2b\rho_x \cos(\psi_1) + 2b\rho_y \sin(\psi_1) + \rho^2 = 0.$$

If $\rho \neq 0$, then it is possible to divide by $2b\rho$ and, by interpreting the equation as the expansion of the cosine of the difference of angles, we get

$$\psi_1 = \tau + \mu.$$

where $\tau = \arctan_2(\rho_y, \rho_x)$ and $\mu = \pm \arccos\left(\frac{-\rho}{2b}\right)$.

If, instead, $\rho = 0$, then the loop equations reduce to

$$\begin{aligned} b\cos(\psi_1) &= b\cos(\psi_2) \\ b\sin(\psi_1) &= b\sin(\psi_2) \end{aligned}$$

that is, infinite solutions exist, all characterized by having the links of length b parallel ($\psi_1 = \psi_2$). Any of such solutions is clearly singular, as the platform can undergo infinitesimal translations in the direction orthogonal to the distal links of the actuated legs.

Given an actuated joint configuration (θ_1, θ_2), for each solution of ψ_1, there exists a single platform configuration, namely

$$\begin{aligned} x &= a\cos(\theta_1) + b\cos(\psi_1) \\ y &= a\sin(\theta_1) + b\sin(\psi_1). \end{aligned}$$

For each input joint configuration, therefore, there are (maximum) two platform positions. If the relationship between the input and output velocities is expressed again as

$$\boldsymbol{J}_w \dot{\boldsymbol{w}} = \boldsymbol{J}_q \dot{\boldsymbol{q}} \tag{10}$$

with $\boldsymbol{w} = [x \quad y]^T$ and $\boldsymbol{q} = [\theta_1 \quad \theta_2]^T$, then these two solutions must have a different value of the sign of $\det(\boldsymbol{J}_w)$, and are therefore separated by a singularity. This can be proved directly as follows. Defining the vector quantities

$$\begin{aligned} \boldsymbol{v} &= [\dot{x} \quad \dot{y} \quad 0]^T \\ \boldsymbol{z} &= [0 \quad 0 \quad 1]^T \end{aligned}$$

and

$$\begin{aligned}\boldsymbol{a}_i &= [a\cos(\theta_i) \quad a\sin(\theta_i) \quad 0]^T = [a_{x,i} \quad a_{y,i} \quad 0]^T \\ \boldsymbol{b}_i &= [b\cos(\psi_i) \quad b\sin(\psi_i) \quad 0]^T = [b_{x,i} \quad b_{y,i} \quad 0]^T\end{aligned}$$

for $i \in \{1, 2\}$, the following identity can be written

$$\boldsymbol{v} = \dot{\theta}_i(\boldsymbol{z} \times \boldsymbol{a}_i) + \dot{\psi}_i(\boldsymbol{z} \times \boldsymbol{a}_i).$$

By taking the dot product of each member with $\boldsymbol{b}_i$, it is possible to cancel the term $\dot{\psi}_i(\boldsymbol{z} \times \boldsymbol{a}_i)$ and determine the matrices of Eq. 10:

$$\boldsymbol{J}_w = \begin{bmatrix} b_{x,1} & b_{y,1} \\ b_{x,2} & b_{y,2} \end{bmatrix}$$

$$\boldsymbol{J}_q = \begin{bmatrix} a_{x,1}b_{y,1} - a_{y,1}b_{x,1} & 0 \\ 0 & a_{x,2}b_{y,2} - a_{y,2}b_{x,2} \end{bmatrix}.$$

It follows that

$$\det(\boldsymbol{J}_w) = b\sin(\psi_2 - \psi_1).$$

This expression can be further simplified by determining ψ_2. In particular, remembering that $\psi_1 = \tau + \mu$ and noticing that $\rho_x = \rho\cos(\tau)$ and $\rho_y = \rho\sin(\tau)$, the two equations Eq. 8 and Eq. 9 can be rewritten as

$$\begin{aligned}\cos(\tau + \mu) + -2\frac{-\rho\cos(\tau)}{2b} &= \cos(\psi_2) \\ \sin(\tau + \mu) + -2\frac{-\rho\sin(\tau)}{2b} &= \sin(\psi_2).\end{aligned}$$

By the definition of μ we have $\cos(\mu) = \frac{-\rho}{2b}$ and thus

$$\begin{aligned}\cos(\psi_2) &= -(\sin(\tau)\sin(\mu) + \cos(\tau)\cos(\mu)) = \cos(\tau - \mu + \pi) \\ \sin(\psi_2) &= \cos(\tau)\sin(\mu) - \sin(\tau)\cos(\mu) = \sin(\tau - \mu + \pi)\end{aligned}$$

from which we obtain $\psi_2 = \tau - \mu + \pi$ and thus

$$\det(\boldsymbol{J}_w) = b\sin(\psi_2 - \psi_1) = b\sin(2\mu).$$

This clearly shows that if the actuated joints do not lead to a singular configuration, the two configurations that the platform can assume have opposite values of $\det(\boldsymbol{J}_w)$, and cannot therefore be joined by a nonsingular assembly mode transition.

8. Purely translational manipulator with nonsingular assembly mode transitions

In the previous section, it was shown that for a $2-\underline{R}RR$ manipulator with a constraining passive leg that limits the motion to pure translations nonsingular assembly mode transitions are impossible. Purely translational 2-DOF mechanisms that undergo nonsingular assembly mode transitions can however be constructed. This can be done by leveraging on the results obtained in the first part of the paper. Let us consider the manipulator shown in Fig. 15. This structure can be derived considering the platform $C_0C_1C_2$ of Fig. 1 as a simple link, and attaching a new rotational joint D_0 to this link. A new platform can then be attached to this new rotational joint D_0 and to a new passive constraining leg λ_3, χ_3 that forces the platform movement to be purely translational. Let us suppose the joint D_0 is placed at distance d from C_0 along the direction which previously corresponded to the y-axis of the platform. Assuming the new reference frame for the platform location is parallel to the base reference frame, and with origin in D_0, the output of the manipulator is given by

$$\begin{bmatrix} x \\ y \end{bmatrix} = \begin{bmatrix} d\cos(\phi) \\ h + d\sin(\phi) \end{bmatrix}.$$

The relationship between the velocities of the new platform and the old platform is clearly

$$\begin{bmatrix} 1 & 0 \\ 0 & 1 \end{bmatrix} \begin{bmatrix} \dot{x} \\ \dot{y} \end{bmatrix} = \begin{bmatrix} -d\sin(\phi) & 0 \\ d\cos(\phi) & 1 \end{bmatrix} \begin{bmatrix} \dot{\phi} \\ \dot{h} \end{bmatrix}$$

and therefore if the manipulator previously studied does not encounter a singular configuration, neither does the new one. The previously shown nonsingular assembly mode transition corresponds therefore to a nonsingular assembly mode transition for the manipulator of Fig. 15.

9. Conclusions

In this paper, the existence of nonsingular assembly mode transitions in 2-DOF manipulators was investigated. First, it was proved that these transitions can occur in manipulators whose range of motions include translation along a fixed direction and rotation of the platform. This was done

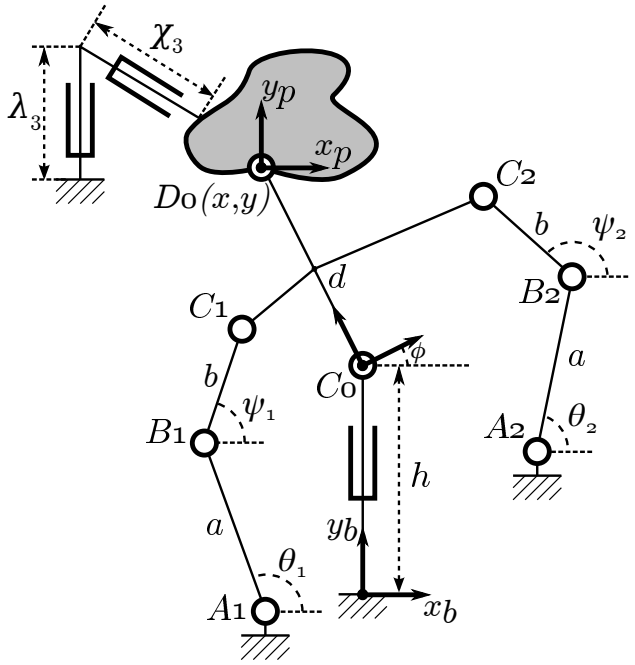

Figure 15: A 2-DOF mechanism capable of nonsingular assembly mode transitions.

by introducing a novel 2-DOF manipulator, actuated by two RRR legs and constrained by a third passive leg that allows only the chosen motions.

The inverse and direct kinematic problems for this manipulator were solved. The maximum number of direct kinematic solutions was proved to be six, and examples of configurations actually exhibiting six real distinct solutions were given. Analysis of direct and inverse kinematics was provided, and a geometrical interpretation of the singularities was given.

An example of dimensioning of the manipulator that presents cusps in the singularity loci was then studied. It was shown that it is possible to perform a nonsingular assembly mode transition by encircling one of these cusps. In particular, the transition can be performed by a pure platform rotation followed by a pure platform translation. We believe this is one of the simplest examples of nonsingular assembly mode transitions ever shown in literature. The configuration studied, therefore, could prove to be valuable as a first benchmark for numerical methods that automatically identify nonsingular changes of assembly mode.

It was then proved that if the passive leg of the manipulator is modified

to allow only translations, nonsingular assembly mode transitions become impossible. Finally, it was shown that, in general, planar mechanisms constrained to pure translations *can* perform nonsingular assembly mode transitions.

This observations leads to two diametrical lines of future work. On the one hand, it would be interesting to extend the proof of non-existence of nonsingular transitions reported in Section 7 to a wider class of planar 2-DOF manipulators. On the other hand, the manipulator of Fig. 15 motivates the pursue for the simplest 2-DOF purely translational manipulator for which nonsingular assembly mode transitions can occur. Additionally, definition of conditions under which nonsingular transitions are impossible for 2-DOF manipulators capable of platform rotations could extend the results presented here to complete the view of the behavior of nonsingular assembly mode transitions in 2-DOF mechanisms.

[1] D. Stewart, A platform with six degrees of freedom, Proc. of the Institution of Mechanical Engineers 180 (1) (1965) 371–386.

[2] V. Gough, S. Whitehall, Universal tyre test machine, in: Proc. FISITA 9th Int. Technical Congress, London, UK, 1962, pp. 117–137.

[3] Y. Tsumaki, H. Naruse, D. N. Nenchev, M. Uchiyama, Design of a compact 6-dof haptic interface, in: 1998 IEEE Int. Conf. on Robotics and Automation (ICRA 1998), Leuven, Belgium, 1998, pp. 2580–2585.

[4] R. Clavel, DELTA, a fast robot with parallel geometry, in: 18th Int. Symp. on Industrial Robots, Lausanne, Switzerland, 1988, pp. 91–100.

[5] F. Pierrot, V. Nabat, O. Company, S. Krut, P. Poignet, Optimal design of a 4-DOF parallel manipulator: From academia to industry, IEEE Transactions on Robotics 25 (2) (2009) 213–224.

[6] C. Gosselin, J. Angeles, Singularity analysis of closed-loop kinematic chains, IEEE Transactions on Robotics 6 (3) (1990) 281–290.

[7] D. Zlatanov, R. G. Fenton, B. Benhabib, Singularity analysis of mechanisms and robots via a motion-space model of the instantaneous kinematics, in: 1994 IEEE Int. Conf. on Robotics and Automation (ICRA 1994), San Diego, CA, USA, 1994, pp. 980–985.

[8] S. Caro, G. Moroz, T. Gayral, D. Chablat, C. Chen, Singularity analysis of a six-dof parallel manipulator using grassmann-cayley algebra and gröebner bases, in: J. Angeles, B. Boulet, J. Clark, J. Kövecses, K. Siddiqi (Eds.), Brain, Body and Machine, Advances in Intelligent and Soft Computing, Springer, Berlin, Heidelberg, 2010, pp. 341–352.

[9] K. J. Waldron, K. H. Hunt, Series-parallel dualities in actively coordinated mechanisms, The International Journal of Robotics Research 10 (5) (1991) 473–480.

[10] F. Gosselin, J.-P. Lallemand, A new insight into the duality between serial and parallel non-redundant and redundant manipulators, Robotica 19 (4) (2001) 365–370.

[11] C. Collins, G. Long, On the duality of twist/wrench distributions in serial and parallel chain robot manipulators, in: 1995 IEEE Int. Conf. on Robotics and Automation (ICRA 1995), Nagoya, Japan, 1995, pp. 526–531.

[12] V. Parenti-Castelli, C. Innocenti, Position analysis of robot manipulators: Regions and subregions, in: Proc. Int. Conf. on Advances in Robot Kinematics, Ljubljana, Yugoslavia, 1988, pp. 150–158.

[13] J. W. Burdick, A classification of 3R regional manipulator singularities and geometries, Mechanism and Machine Theory 30 (1) (1995) 71–89.

[14] J. Omri, P. Wenger, A general criterion for the identification of nonsingular posture changing 3-DOF manipulators, in: J.-P. Merlet, B. Ravani (Eds.), Computational Kinematics 95, Vol. 40 of Solid Mechanics and Its Applications, Springer, Netherlands, 1995, pp. 153–162.

[15] M. Husty, J. Schadlbauer, S. Caro, P. Wenger, The 3-rps manipulator can have non-singular assembly-mode changes, in: F. Thomas, A. Perez Gracia (Eds.), Computational Kinematics, Vol. 15 of Mechanisms and Machine Science, Springer Netherlands, 2014, pp. 339–348.

[16] S. Caro, P. Wenger, D. Chablat, Non-singular assembly mode changing trajectories of a 6-dof parallel robot, in: Proceedings of the ASME 2012 International Design Engineering Technical Conferences & Computers and Information in Engineering Conference, Chicago,IL,USA, 2012, pp. 1–10.

[17] P. R. McAree, R. W. Daniel, An explanation of never-special assembly changing motions for 3–3 parallel manipulators, The International Journal of Robotics Research 18 (6) (1999) 556–574.

[18] H. Bamberger, A. Wolf, M. Shoham, Assembly mode changing in parallel mechanisms, IEEE Transactions on Robotics 24 (4) (2008) 765–772.

[19] D. Chablat, P. Wenger, Séparation des solutions aux modèles géométriques direct et inverse pour les manipulateurs pleinement parallèles, Mechanism and Machine Theory 36 (6) (2001) 763–783.

[20] E. Macho, O. Altuzarra, V. Petuya, A. Hernandez, Workspace enlargement merging assembly modes. Application to the 3-RRR planar platform, International Journal of Mechanics and Control 10 (1) (2009) 13–20.

[21] C. M. Gosselin, J. Wang, Singularity loci of planar parallel manipulators with revolute actuators, Robotics and Autonomous Systems 21 (4) (1997) 377–398.

[22] I. A. Bonev, C. M. Gosselin, Singularity loci of planar parallel manipulators with revolute joints, in: Proc. of the 2nd Workshop on Computational Kinematics, 2001, pp. 291–299.

[23] I. A. Bonev, D. Zlatanov, C. M. Gosselin, Singularity analysis of 3-DOF planar parallel mechanisms via screw theory, Journal of Mechanical Design 125 (2003) 573.

[24] J. Sefrioui, C. M. Gosselin, On the quadratic nature of the singularity curves of planar three-degree-of-freedom parallel manipulators, Mechanism and Machine Theory 30 (4) (1995) 533–551.

[25] X. Kong, C. M. Gosselin, Forward displacement analysis of third-class analytic 3-RPR planar parallel manipulators, Mechanism and Machine Theory 36 (9) (2001) 1009–1018.

[26] M. Coste, A simple proof that generic 3-RPR manipulators have two aspects, Journal of Mechanisms and Robotics 4 (1) (2012) 011008.

[27] M. Zein, P. Wenger, D. Chablat, Non-singular assembly-mode changing motions for 3-RPR parallel manipulators, Mechanism and Machine Theory 43 (4) (2008) 480–490.

[28] P. Wenger, D. Chablat, Workspace and assembly modes in fully-parallel manipulators: A descriptive study, in: J. Lenarčič, M. L. Husty (Eds.), Advances in Robot Kinematics: Analysis and Control, Kluwer Academic Publishers, Netherlands, 1998, pp. 117–126.

[29] M. Zein, P. Wenger, D. Chablat, Singular curves in the joint space and cusp points of 3-RPR parallel manipulators, Robotica 25 (6) (2007) 717–724.

[30] M. L. Husty, Non-singular assembly mode change in 3-RPR-parallel manipulators, in: A. Kecskemthy, A. Mller (Eds.), Computational Kinematics, Springer Berlin Heidelberg, 2009, pp. 51–60.

[31] A. K. Zaiter, P. Wenger, D. Chablat, A study of the singularity locus in the joint space of planar parallel manipulators: special focus on cusps and nodes, in: Int. Congress Design and Modeling of Mechanical Systems, Sousse, Tunisia, 2011, pp. 1–8.

[32] X. Kong, C. Gosselin, Determination of the uniqueness domains of 3-RPR planar parallel manipulators with similar platforms, in: Proc. of the 2000 ASME Design Engineering Technical conferences and Computers and Information in Engineering Conf., Montreal, Canada, 2000, pp. 10–13.

[33] P. Wenger, D. Chablat, M. Zein, Degeneracy study of the forward kinematics of planar 3-RPR parallel manipulators, Journal of Mechanical Design 129 (12) (2007) 1265–1268.

[34] P. Wenger, D. Chablat, Kinematic analysis of a class of analytic planar 3-RPR parallel manipulators, in: A. Kecskeméthy, A. Mèuller (Eds.), Computational Kinematics, Springer, Berlin, Heidelberg, 2009, pp. 43–50.

[35] M. Urizar, V. Petuya, O. Altuzarra, A. Hernandez, Assembly mode changing in the cuspidal analytic 3-RPR, IEEE Transactions on Robotics 28 (2) (2012) 506–513.

[36] D. Chablat, G. Moroz, V. Arakelian, S. Briot, P. Wenger, Solution regions in the parameter space of a 3-RRR decoupled robot for a prescribed workspace, in: J. Lenarcic, M. Husty (Eds.), Latest Advances in Robot Kinematics, Springer, Netherlands, 2012, pp. 357–364.

[37] C. Gosselin, J. Angeles, The optimum kinematic design of a planar three-degree-of-freedom parallel manipulator, Journal of Mechanisms, Transmissions, and Automation in Design 110 (1) (1988) 35–41.

[38] D. Chablat, P. Wenger, The kinematic analysis of a symmetrical three-degree-of-freedom planar parallel manipulator, in: CISM-IFToMM Symp. on Robot Design, Dynamics and Control, Montreal, Canada, 2004.

[39] E. Macho, O. Altuzarra, C. Pinto, A. Hernandez, Transitions between multiple solutions of the direct kinematic problem, in: J. Lenari, P. Wenger (Eds.), Advances in Robot Kinematics: Analysis and Design, Springer, Netherlands, 2008, pp. 301–310.

[40] A. Hernandez, O. Altuzarra, V. Petuya, E. Macho, Defining conditions for nonsingular transitions between assembly modes, IEEE Transactions on Robotics 25 (6) (2009) 1438–1447.

[41] V. Arakelian, S. Briot, S. Yatsun, A. Yatsun, A new 3-DoF planar parallel manipulator with unlimited rotation capability, in: Proc.of the 13th World Congress in Robot and Machine Science, Guanajuato, Mexico, 2011, pp. IMD–123.

[42] F. Gao, X. Liu, W. A. Gruver, Performance evaluation of two-degree-of-freedom planar parallel robots, Mechanism and Machine Theory 33 (6) (1998) 661–668.

[43] D. Chablat, P. Wenger, Working modes and aspects in fully parallel manipulators, in: 1998 IEEE Int. Conf. on Robotics and Automation (ICRA 1998), Leuven, Belgium, 1998, pp. 1964–1969.

[44] J. J. Cervantes-Sánchez, J. C. Hernández-Rodríguez, J. G. Rendón-Sánchez, On the workspace, assembly configurations and singularity curves of the RRRRR-type planar manipulator, Mechanism and Machine Theory 35 (8) (2000) 1117–1139.

[45] J. Wu, J. Wang, L. Wang, A comparison study of two planar 2-DOF parallel mechanisms: one with 2-RRR and the other with 3-RRR structures, Robotica 28 (6) (2010) 937–942.

[46] T. Huang, M. Li, Z. Li, D. Chetwynd, D. Whitehouse, Optimal kinematic design of 2-DOF parallel manipulators with well-shaped workspace bounded by a specified conditioning index, IEEE Transactions on Robotics and Automation 20 (3) (2004) 538–543.

[47] X.-J. Liu, J. Wang, G. Pritschow, On the optimal kinematic design of the PRRRP 2-DoF parallel mechanism, Mechanism and Machine Theory 41 (9) (2006) 1111–1130.

[48] T. Huang, Z. Li, M. Li, D. G. Chetwynd, C. M. Gosselin, Conceptual design and dimensional synthesis of a novel 2-DOF translational parallel robot for pick-and-place operations, Journal of Mechanical Design 126 (2004) 449.

[49] M. M. Da Silva, L. P. de Oliveira, O. Brüls, M. Michelin, C. Baradat, O. Tempier, J. De Caigny, J. Swevers, W. Desmet, H. Van Brussel, Integrating structural and input design of a 2-DOF high-speed parallel manipulator: A flexible model-based approach, Mechanism and Machine Theory 45 (11) (2010) 1509–1519.

[50] D. Zhang, C. Gosselin, Kinetostatic modeling of parallel mechanisms with a passive constraining leg and revolute actuators, Mechanism and Machine Theory 37 (6) (2002) 599 – 617.

[51] Y. Lu, Y. Shi, S.-H. Li, X.-B. Tian, Synthesis and analysis of kinematics/statics of a novel 2SPS+ SPR+ SP parallel manipulator, Journal of Mechanical Design 130 (2008) 092302.

[52] X. Kong, C. M. Gosselin, Generation and forward displacement analysis of rpr-pr-rpr analytic planar parallel manipulators, Journal of Mechanical Design 124 (2002) 294.

[53] M. Manubens, G. Moroz, D. Chablat, F. Rouillier, P. Wenger, Cusp points in the parameter space of degenerate 3-rpr planar parallel manipulators, Journal of Mechanisms and Robotics 4 (2012) 041003.

[54] X. Kong, C. M. Gosselin, A formula that produces a unique solution to the forward displacement analysis of a quadratic spherical parallel manipulator: The agile eye, Journal of Mechanisms and Robotics 2 (2010) 044501.